

INTERNATIONAL STANDARD



BASIC EMC PUBLICATION

**Electromagnetic compatibility (EMC) –
Part 2-10: Environment – Description of HEMP environment – Conducted
disturbance**





THIS PUBLICATION IS COPYRIGHT PROTECTED
Copyright © 2021 IEC, Geneva, Switzerland

All rights reserved. Unless otherwise specified, no part of this publication may be reproduced or utilized in any form or by any means, electronic or mechanical, including photocopying and microfilm, without permission in writing from either IEC or IEC's member National Committee in the country of the requester. If you have any questions about IEC copyright or have an enquiry about obtaining additional rights to this publication, please contact the address below or your local IEC member National Committee for further information.

IEC Central Office
3, rue de Varembé
CH-1211 Geneva 20
Switzerland

Tel.: +41 22 919 02 11
info@iec.ch
www.iec.ch

About the IEC

The International Electrotechnical Commission (IEC) is the leading global organization that prepares and publishes International Standards for all electrical, electronic and related technologies.

About IEC publications

The technical content of IEC publications is kept under constant review by the IEC. Please make sure that you have the latest edition, a corrigendum or an amendment might have been published.

IEC publications search - webstore.iec.ch/advsearchform

The advanced search enables to find IEC publications by a variety of criteria (reference number, text, technical committee, ...). It also gives information on projects, replaced and withdrawn publications.

IEC Just Published - webstore.iec.ch/justpublished

Stay up to date on all new IEC publications. Just Published details all new publications released. Available online and once a month by email.

IEC Customer Service Centre - webstore.iec.ch/csc

If you wish to give us your feedback on this publication or need further assistance, please contact the Customer Service Centre: sales@iec.ch.

IEC online collection - oc.iec.ch

Discover our powerful search engine and read freely all the publications previews. With a subscription you will always have access to up to date content tailored to your needs.

Electropedia - www.electropedia.org

The world's leading online dictionary on electrotechnology, containing more than 22 000 terminological entries in English and French, with equivalent terms in 18 additional languages. Also known as the International Electrotechnical Vocabulary (IEV) online.



IEC 61000-2-10

Edition 2.0 2021-11

INTERNATIONAL STANDARD



BASIC EMC PUBLICATION

**Electromagnetic compatibility (EMC) –
Part 2-10: Environment – Description of HEMP environment – Conducted
disturbance**

IECNORM.COM : Click to view the full PDF of IEC 61000-2-10:2021

INTERNATIONAL
ELECTROTECHNICAL
COMMISSION

ICS 33.100.01

ISBN 978-2-8322-1050-6

Warning! Make sure that you obtained this publication from an authorized distributor.

CONTENTS

FOREWORD	5
INTRODUCTION	7
1 Scope	8
2 Normative references	8
3 Terms and definitions	8
4 General	12
5 Description of HEMP environment, conducted parameters	13
5.1 Introductory remarks	13
5.2 Early-time HEMP external conducted environment	13
5.3 Intermediate-time HEMP external conducted environment	15
5.4 Late-time HEMP external conducted environment	15
5.5 Antenna currents	17
5.6 HEMP internal conducted environments	21
Annex A (informative) Discussion of early-time HEMP coupling for long lines	23
A.1 Elevated line coupling	23
A.2 Buried line coupling	24
Annex B (informative) Discussion of intermediate-time HEMP coupling for long lines	26
B.1 General	26
B.2 Elevated line coupling	26
B.3 Buried line coupling	26
Annex C (informative) Responses of simple linear antennas to the IEC early-time HEMP environment	28
C.1 Overview	28
C.2 IEC early-time HEMP environment	28
C.3 Evaluation of the antenna responses	31
C.3.1 General	31
C.3.2 Monopole antenna	31
C.3.3 Dipole antenna	32
C.4 Calculated results	33
C.5 Summary of results	34
Annex D (informative) Measured cable currents inside telephone buildings	43
Annex E (informative) Time waveform description for the responses of simple linear antennas to the early-time HEMP environment	44
E.1 General	44
E.2 Description of the recommended waveform	44
E.3 Procedure for determining the test waveform	46
Bibliography	47
Figure 1 – Geometry for the definition of polarization and of the angles of elevation ψ and azimuth ϕ	9
Figure 2 – Geometry for the definition of the plane wave	10
Figure 3 – Geomagnetic dip angle	11
Figure 4 – Three-phase line and equivalent circuit for computing late-time HEMP conducted current	16

Figure 5 – Centre-loaded dipole antenna of length l and radius a , excited by an incident early-time HEMP field	18
Figure A.1 – Variation of peak coupled cable current versus local geomagnetic dip angle	23
Figure C.1 – Illustration of the incident HEMP field	29
Figure C.2 – HEMP tangent radius R_t defining the illuminated region, shown as a function of burst height (HOB)	29
Figure C.3 – Geometry of the monopole antenna	32
Figure C.4 – Geometry of the dipole antenna	33
Figure C.5 – Cumulative probability distributions for the peak responses for the 1 m vertical monopole antenna load currents and voltages	34
Figure C.6 – Cumulative probability distributions for the peak responses for the 3 m vertical monopole antenna load currents and voltages	35
Figure C.7 – Cumulative probability distributions for the peak responses for the 10 m vertical monopole antenna load currents and voltages	36
Figure C.8 – Cumulative probability distributions for the peak responses for the 100 m vertical monopole antenna load currents and voltages	37
Figure C.9 – Cumulative probability distributions for the peak responses for the 1 m horizontal dipole antenna load currents and voltages	38
Figure C.10 – Cumulative probability distributions for the peak responses for the 3 m horizontal dipole antenna load currents and voltages	39
Figure C.11 – Cumulative probability distributions for the peak responses for the 10 m horizontal dipole antenna load currents and voltages	40
Figure C.12 – Cumulative probability distributions for the peak responses for the 100 m horizontal dipole antenna load current and voltages	41
Figure C.13 – Plot of multiplicative correction factors for correcting the values of V_{oc} , I_{sc} , I_L and V_L for antennas having other L/a ratios	42
Figure E.1 – Comparison of a computation and an analytic formula for a 1 m wire illuminated by the E_1 HEMP with the field parallel to the wire (and no ground present) [11] ..	45
Figure E.2 – General waveform of the damped oscillatory waveform from IEC 61000-4-18 [14]	45
Table 1 – Early-time HEMP conducted common-mode short-circuit currents including the time history and peak value I_{pk} as a function of severity level, length L (in metres) and ground conductivity σ_g	14
Table 2 – Intermediate-time HEMP conducted common-mode short-circuit currents including the time history and peak value I_{pk} as a function of length L (in metres) and ground conductivity σ_g	15
Table 3 – Maximum peak electric dipole antenna load current versus frequency for antenna principal frequencies	19
Table 4 – HEMP response levels for V_{oc} for the vertical monopole antenna	19
Table 5 – HEMP response levels for I_{sc} for the vertical monopole antenna	20
Table 6 – HEMP response levels for I_L for the loaded vertical monopole antenna ^a	20
Table 7 – HEMP response levels for V_{oc} for the horizontal dipole antenna	20
Table 8 – HEMP response levels for I_{sc} for the horizontal dipole antenna	21
Table 9 – HEMP response levels for I_L for the loaded horizontal dipole antenna ^a	21

Table A.1 – Rectified impulse (RI) and computed effective pulse widths for vertical polarization of the early-time HEMP for an elevated conductor ($h = 10$ m).....	24
Table A.2 – Coupled early-time HEMP currents for a buried conductor ($z = -1$ m).....	25
Table A.3 – Waveform parameters for early-time HEMP buried conductor coupling ($z = -1$ m)	25
Table A.4 –Average waveform parameters for early-time HEMP buried conductor currents	25
Table B.1 – Coupled HEMP intermediate-time short-circuit currents for an elevated conductor ($h = 10$ m).....	26
Table B.2 – Coupled HEMP intermediate-time short-circuit currents for a buried conductor ($h = -1$ m)	26
Table D.1 – Estimated internal peak-to-peak cable currents (I_{PP}) from direct HEMP illumination (from [8])	43
Table D.2 – Damped sinusoid waveform characteristics for internal cable currents (measured) (from [8])	43
Table E.1 – Waveform parameters to be used in Formula (E.1).....	46

IECNORM.COM : Click to view the full PDF of IEC 61000-2-10:2021

INTERNATIONAL ELECTROTECHNICAL COMMISSION

ELECTROMAGNETIC COMPATIBILITY (EMC) –**Part 2-10: Environment – Description of HEMP environment –
Conducted disturbance****FOREWORD**

1) The International Electrotechnical Commission (IEC) is a worldwide organization for standardization comprising all national electrotechnical committees (IEC National Committees). The object of IEC is to promote international co-operation on all questions concerning standardization in the electrical and electronic fields. To this end and in addition to other activities, IEC publishes International Standards, Technical Specifications, Technical Reports, Publicly Available Specifications (PAS) and Guides (hereafter referred to as "IEC Publication(s)"). Their preparation is entrusted to technical committees; any IEC National Committee interested in the subject dealt with may participate in this preparatory work. International, governmental and non-governmental organizations liaising with the IEC also participate in this preparation. IEC collaborates closely with the International Organization for Standardization (ISO) in accordance with conditions determined by agreement between the two organizations.

2) The formal decisions or agreements of IEC on technical matters express, as nearly as possible, an international consensus of opinion on the relevant subjects since each technical committee has representation from all interested IEC National Committees.

3) IEC Publications have the form of recommendations for international use and are accepted by IEC National Committees in that sense. While all reasonable efforts are made to ensure that the technical content of IEC Publications is accurate, IEC cannot be held responsible for the way in which they are used or for any misinterpretation by any end user.

4) In order to promote international uniformity, IEC National Committees undertake to apply IEC Publications transparently to the maximum extent possible in their national and regional publications. Any divergence between any IEC Publication and the corresponding national or regional publication shall be clearly indicated in the latter.

5) IEC itself does not provide any attestation of conformity. Independent certification bodies provide conformity assessment services and, in some areas, access to IEC marks of conformity. IEC is not responsible for any services carried out by independent certification bodies.

6) All users should ensure that they have the latest edition of this publication.

7) No liability shall attach to IEC or its directors, employees, servants or agents including individual experts and members of its technical committees and IEC National Committees for any personal injury, property damage or other damage of any nature whatsoever, whether direct or indirect, or for costs (including legal fees) and expenses arising out of the publication, use of, or reliance upon, this IEC Publication or any other IEC Publications.

8) Attention is drawn to the Normative references cited in this publication. Use of the referenced publications is indispensable for the correct application of this publication.

9) Attention is drawn to the possibility that some of the elements of this IEC Publication may be the subject of patent rights. IEC shall not be held responsible for identifying any or all such patent rights.

IEC 61000-2-10 has been prepared by subcommittee 77C: High power transient phenomena, of IEC technical committee 77: Electromagnetic compatibility. It is an International Standard.

It forms Part 2-10 of IEC 61000. It has the status of a basic EMC publication in accordance with IEC Guide 107.

This second edition cancels and replaces the first edition published in 1998. This edition constitutes a technical revision.

This edition includes the following significant technical changes with respect to the previous edition:

- a new Annex E has been added to describe the time waveform characteristics of the response of simple linear antennas to aid in the development of test methods;
- technical support for this waveform is provided in Annex E.

c) a procedure to use the waveforms presented in Annex E along with the peak values previously provided in Annex C is provided.

The text of this International Standard is based on the following documents:

Draft	Report on voting
77C/318/FDIS	77C/321/RVD

Full information on the voting for its approval can be found in the report on voting indicated in the above table.

The language used for the development of this International Standard is English.

This document was drafted in accordance with ISO/IEC Directives, Part 2, and developed in accordance with ISO/IEC Directives, Part 1 and ISO/IEC Directives, IEC Supplement, available at www.iec.ch/members_experts/refdocs. The main document types developed by IEC are described in greater detail at www.iec.ch/standardsdev/publications.

A list of all parts in the IEC 61000 series, published under the general title *Electromagnetic compatibility*, can be found on the IEC website.

The committee has decided that the contents of this document will remain unchanged until the stability date indicated on the IEC website under webstore.iec.ch in the data related to the specific document. At this date, the document will be

- reconfirmed,
- withdrawn,
- replaced by a revised edition, or
- amended.

IMPORTANT – The "colour inside" logo on the cover page of this document indicates that it contains colours which are considered to be useful for the correct understanding of its contents. Users should therefore print this document using a colour printer.

INTRODUCTION

IEC 61000 is published in separate parts according to the following structure:

Part 1: General

General considerations (introduction, fundamental principles)

Definitions, terminology

Part 2: Environment

Description of the environment

Classification of the environment

Compatibility levels

Part 3: Limits

Emission limits

Immunity limits (insofar as these limits do not fall under the responsibility of the product committees)

Part 4: Testing and measurement techniques

Measurement techniques

Testing techniques

Part 5: Installation and mitigation guidelines

Installation guidelines

Mitigation methods and devices

Part 6: Generic standards

Part 9: Miscellaneous

Each part is further subdivided into several parts, published either as international standards or as technical specifications or technical reports, some of which have already been published as sections. Others will be published with the part number followed by a dash and a second number identifying the subdivision (example: IEC 61000-6-1).

The IEC has initiated the preparation of standardized methods to protect civilian society from the effects of high-power electromagnetic environments including the high-altitude electromagnetic pulse. Such environments could disrupt systems for communications, electric power, information technology, etc.

This part of IEC 61000 is an international standard that establishes the HEMP conducted disturbances that are the result of coupling by the radiated HEMP disturbances.

ELECTROMAGNETIC COMPATIBILITY (EMC) –

Part 2-10: Environment – Description of HEMP environment – Conducted disturbance

1 Scope

This part of IEC 61000 defines the high-altitude electromagnetic pulse (HEMP) conducted environment that is one of the consequences of a high-altitude nuclear explosion.

Those dealing with this subject consider two cases:

- high-altitude nuclear explosions;
- low-altitude nuclear explosions.

For civil systems the most important case is the high-altitude nuclear explosion. In this case, the other effects of the nuclear explosion such as blast, ground shock, thermal and nuclear ionizing radiation are not present at the ground level.

However, the electromagnetic pulse associated with the explosion can cause disruption of, and damage to, communication, electronic and electric power systems thereby upsetting the stability of modern society.

The object of this document is to establish a common reference for the conducted HEMP environment in order to select realistic stresses to apply to victim equipment to evaluate their performance.

2 Normative references

The following documents are referred to in the text in such a way that some or all of their content constitutes requirements of this document. For dated references, only the edition cited applies. For undated references, the latest edition of the referenced document (including any amendments) applies.

IEC 61000-2-9, *Electromagnetic compatibility (EMC) – Part 2: Environment – Section 9: Description of HEMP environment – Radiated disturbance*

IEC 61000-4-24, *Electromagnetic compatibility (EMC) – Part 4-24: Testing and measurement techniques – Test methods for protective devices for HEMP conducted disturbance*

3 Terms and definitions

For the purposes of this document, the following terms and definitions apply.

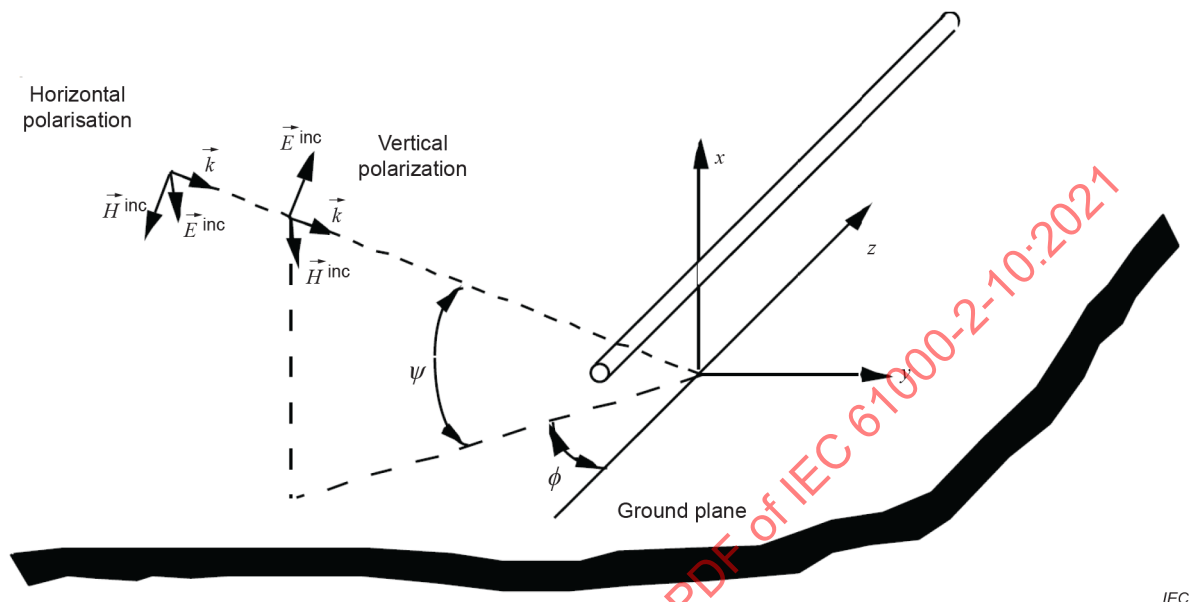
ISO and IEC maintain terminological databases for use in standardization at the following addresses:

- IEC Electropedia: available at <http://www.electropedia.org/>
- ISO Online browsing platform: available at <http://www.iso.org/obp>

3.1**angle of elevation ψ**

angle ψ measured in the vertical plane between a flat horizontal surface such as the ground and the propagation vector

SEE: Figure 1.



IEC

Figure 1 – Geometry for the definition of polarization and of the angles of elevation ψ and azimuth ϕ

3.2**azimuth angle ϕ**

angle between the projection of the propagation vector on the ground plane and the principal axis of the victim object

Note 1 to entry: It is the z axis for the transmission line of Figure 1.

3.3**composite waveform**

waveform which maximizes the important features of a waveform

3.4**coupling**

interaction of the HEMP field with a system to produce currents and voltages on system surfaces and cables

Note 1 to entry: Voltages result from the induced charges and are only defined at low frequencies with wavelengths larger than the surface or gap dimensions

3.5**direction of propagation of the electromagnetic wave**

direction of the propagation vector \vec{k} , perpendicular to the plane containing the vectors of the electric and magnetic fields

Note 1 to entry: See Figure 2.

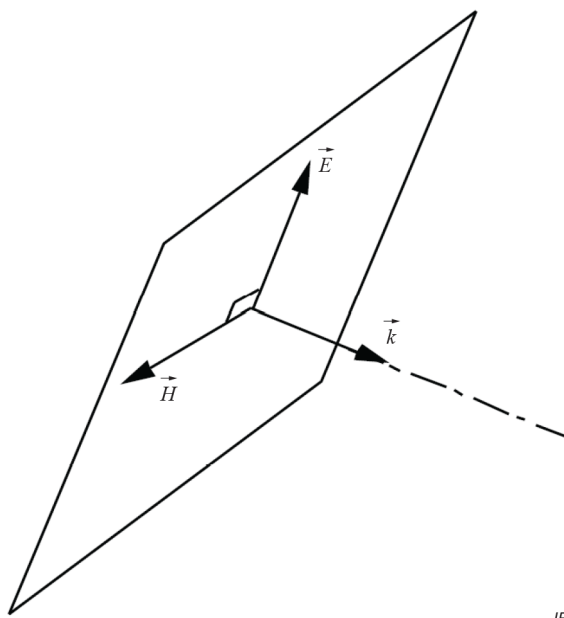


Figure 2 – Geometry for the definition of the plane wave

3.6

E1

early-time HEMP electric field

3.7

E2

intermediate-time HEMP electric field

3.8

E3

late-time HEMP electric field

3.9

electromagnetic pulse

EMP

any electromagnetic field waveform abruptly rising and falling in the time domain created by a nuclear detonation at any altitude

3.10

geomagnetic dip angle

θ_{dip}

dip angle of the geomagnetic flux density vector \vec{B}_e , measured from the local horizontal in the magnetic north-south plane

Note 1 to entry: $\theta_{\text{dip}} = 90^\circ$ at the magnetic north pole, -90° at the magnetic south pole (see Figure 3).

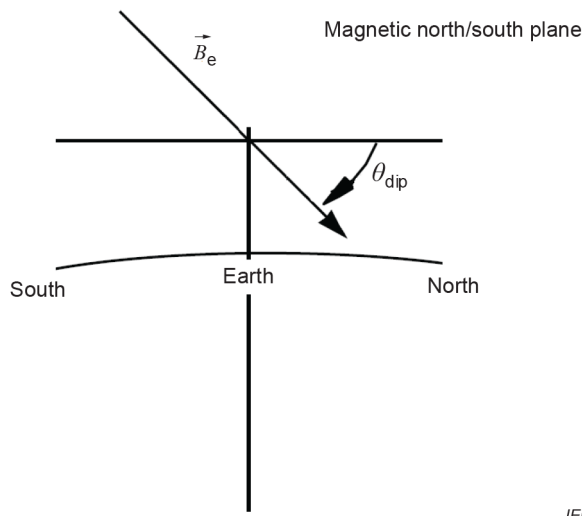


Figure 3 – Geomagnetic dip angle

**3.11
high-altitude electromagnetic pulse
HEMP**

high-altitude electromagnetic pulse created by a high-altitude nuclear explosion

**3.12
high-altitude nuclear explosion**
height of burst above 30 km altitude

**3.13
horizontal polarization**

position of the electromagnetic wave in which the magnetic field vector is in the incidence plane and the electric field vector is perpendicular to the incidence plane and thus parallel to the ground plane

Note 1 to entry: This type of polarization is also called perpendicular or transverse electric (TE) (see Figure 1).

**3.14
incidence plane**
plane formed by the propagation vector and the normal to the ground plane

**3.15
low-altitude nuclear explosion**
height of burst below 1 km altitude

**3.16
NEMP
nuclear EMP**
all types of EMP produced by a nuclear explosion

**3.17
point-of-entry
PoE**
physical location (point) on an electromagnetic barrier, where EM energy can enter or exit a topological volume, unless an adequate PoE protective device is provided

Note 1 to entry: A PoE is not limited to a geometrical point. PoEs are classified as aperture PoEs or conductive PoEs according to the type of penetration. They are also classified as architectural, mechanical, structural or electrical PoEs, according to the functions they serve.

3.18**pulse width**

time interval between the points on the leading and trailing edges of a pulse at which the instantaneous value is 50 % of the peak pulse amplitude, unless otherwise stated

3.19**rectified impulse**

integral of the absolute value of a time waveform's amplitude over a specified time interval

3.20**rise time**

time interval between the instants in which the instantaneous amplitude of a pulse first reaches specified lower and upper limits, namely 10 % and 90 % of the peak pulse amplitude, unless otherwise stated

3.21**short-circuit current**

value of current that flows when the output terminals of a circuit are shorted

Note 1 to entry: This current is normally of interest when checking the performance of surge protection devices.

3.22**source impedance**

impedance presented by a source of energy to the input terminals of a device or network

3.23**vertical polarization**

position of the electromagnetic wave in which the electric field vector is in the incidence plane, and the magnetic field vector is perpendicular to the incidence plane and thus parallel to the ground plane

Note 1 to entry: See Figure 1.

Note 2 to entry: This type of polarization is also called parallel or transverse magnetic (TM).

4 General

A high-altitude (above 30 km) nuclear burst produces three types of electromagnetic pulses which are observed on the earth's surface:

- 1) early-time HEMP (fast);
- 2) intermediate-time HEMP (medium);
- 3) late-time HEMP (slow).

Historically most of the interest has been focused on the early-time HEMP which was previously referred to simply as HEMP. Here the term high-altitude EMP or HEMP will be used to include all three types. The term nuclear electromagnetic pulse (NEMP) covers many categories of nuclear EMPs including those produced by surface bursts (source region EMPs (SREMPs)) or created on space systems (system generated EMPs SGEMPs)).

Because the HEMP is produced by a high-altitude detonation, other nuclear weapon environments such as gamma rays, heat and shock waves at the earth's surface are not observed at the earth's surface. HEMP was reported from high-altitude nuclear tests in the South Pacific by the U.S. and over the USSR during the early 1960s, producing effects on electronic equipment on the ground far from the burst location.

This document presents the conducted HEMP environment induced on metallic lines, such as cables or power lines, external and internal to installations, and external antennas.

5 Description of HEMP environment, conducted parameters

5.1 Introductory remarks

The electromagnetic field generated by a high-altitude nuclear explosion described in IEC 61000-2-9 can induce currents and voltages in all metallic structures. These currents and voltages propagating in conductors represent the conducted environment. This means that the conducted environment is a secondary phenomenon, a consequence of the radiated field alone.

All metallic structures (i.e., wires, conductors, pipes, ducts, etc.) will be affected by the HEMP. The conducted environment is important because it can direct the HEMP energy to sensitive electronics through signal, power, and grounding connections. It should be noted that there are two distinct categories of conductors: external and internal conductors (with regard to a building or any other enclosure). While this can seem simplistic, this separation is critical in terms of the information to be provided in this document.

The difference between these two types of conductors is explained by electromagnetic topology. In general, external conductors are those which are located outside of a building and are completely exposed to the full HEMP environment. This category includes power, metallic communication lines, antenna cables, and water and gas pipes (if metallic). For the purposes of this document, the conductors can be elevated above the ground or buried in the earth. Internal conductors are those which are located in a partially or completely shielded building where the HEMP fields have been reduced by the building. This is a much more complex situation, because the HEMP field waveforms will be significantly altered by the building shield, and the coupling to internal wires and cables is consequently very difficult to calculate, although some measured data are available from simulated HEMP tests.

In this document the external conducted common mode environments are calculated using simplified conductor geometries and the specified HEMP environments for the early, intermediate, and late-time waveforms. These conducted external environments are intended to be used to evaluate the performance of protection devices outside of a building, and because of variations in telecom and power systems, the effects of transformers and telephone splice boxes are not considered here. This process results in approximate, but well-defined waveforms that are needed to test protective elements on external conductors in a standardized manner. For the internal conductors, a procedure is defined to estimate the conducted environments appropriate for equipment testing. For unshielded multiconductor wires, it is assumed that the line-to-ground currents are equal to the common-mode current.

5.2 Early-time HEMP external conducted environment

For the early-time HEMP, the high-amplitude electric field couples efficiently to antennas and to any exposed lines such as power and telephone lines. The antenna coupling mechanism is extremely variable and dependent on the details of the antenna design. In many cases, it is advisable to perform continuous wave (CW) testing of an antenna and to "combine" the response function of the antenna with the incident HEMP environment using a convolution technique. However, simple formulae have been provided to compute the response of thin antennas (see 5.5). For long lines, it is possible to perform a comprehensive set of common mode calculations that are reliable and depend only upon a few parameters. These parameters include conductor length, exposure situation (above ground or buried), and the surface ground conductivity (for depths between 0 m and 5 m). In addition, because the HEMP coupling is dependent on angle of elevation and polarization (see Figure 1), it is possible to statistically examine the probability of producing particular levels of current.

Table 1 describes the calculated, coupled, common-mode short-circuit currents and the Thévenin equivalent source impedances (used to determine the open-circuit voltages) as functions of severity level, length of conductor, and ground conductivity. These results are appropriate for the common-mode currents flowing on bare wires, overhead insulated wires, and the shields of shielded cables or coaxial transmission lines. For shielded cables one should use measured or specified cable transfer impedances to determine internal wire currents and voltages. Although some waveform variation occurs for different exposure geometries, a single time waveform is specified for elevated lines. The waveform is defined in terms of the rise time (10 % to 90 %) and the pulse width (at half maximum); when the pulse characteristics of rise time and pulse width are described together, the usual description is $\Delta t_r/\Delta t_{pw}$.

In Table 1 a severity level of 99 % indicates that 99 % of the currents produced will be less than this value. The buried line currents calculated vary much less with angle of incidence and indicate a very broad probability distribution (small differences between 10 % and 90 % severity) and therefore are not described in terms of severity levels; variations are shown for ground conductivity. In terms of applicability for Table 1, the elevated conductor currents are accurate for heights above 5 m while the buried currents can be used for conductors slightly ($h < 30$ cm) above the surface and below the surface. For conductor heights below 5 m, the values in Table 1 can be linearly interpolated (between 0,3 m and 5 m). For cases where the lines from an elevated geometry enter the ground in an insulated manner, the currents will initially resemble waveform 1, decreasing as a function of burial distance until waveform 2 is reached (requires approximately 20 m). Consult Annex A for further information regarding the derivation of these waveforms.

Table 1 – Early-time HEMP conducted common-mode short-circuit currents including the time history and peak value I_{pk} as a function of severity level, length L (in metres) and ground conductivity σ_g

		Elevated conductor		
		I_{pk} A		
Severity (%) ^a		$L > 200$ m	$100 \leq L \leq 200$ m	$L < 100$ m
50		500	500	$5,0 \times L$
90		1 500	$7,5 \times L$	$7,5 \times L$
99		4 000	$20 \times L$	$20 \times L$

^a Percentage of currents smaller than the indicated value.

Waveform 1: 10/100 ns.

Source impedance: $Z_s = 400 \Omega$.

Buried conductor	
I_{pk} A	
σ_g S/m	All lengths > 10 m
10^{-2}	200
10^{-3}	300
10^{-4}	400

Waveform 2: 25/500 ns.

Source impedance: $Z_s = 50 \Omega$.

5.3 Intermediate-time HEMP external conducted environment

The intermediate-time HEMP environment only couples efficiently to long conductors in excess of 1 km. It is therefore of interest primarily for external conductors such as power and communication lines. Because the pulse width of this environment is much wider than that of the early-time environment, the coupling varies less as a function of angle of elevation. This means that the statistical variation is less important than in the case of the early-time coupling. On the other hand, the ground conductivity is more important here, affecting the coupling to elevated lines in addition to buried lines. See Annex B for a more detailed discussion.

Table 2 describes the conducted external environment as a function of line length and ground conductivity (to depths of 1 km).

Table 2 – Intermediate-time HEMP conducted common-mode short-circuit currents including the time history and peak value I_{pk} as a function of length L (in metres) and ground conductivity σ_g

σ_g S/m	Elevated conductor			
	$L > 10\ 000\ m$	$1\ 000 \leq L \leq 10\ 000\ m$	$100 \leq L \leq 1\ 000\ m$	$L < 100\ m$
10^{-2}	150	75	$0,05 \times L$	0
10^{-3}	350	200	$0,15 \times L$	0
10^{-4}	800	600	$0,45 \times L$	0

Waveform 3: 25/1 500 µs.
Source impedance: $Z_s = 400\ \Omega$.

σ_g S/m	Buried conductor		
	$L > 1\ 000\ m$	$100 \leq L \leq 1\ 000\ m$	$L < 100\ m$
10^{-2}	50	$0,05 \times L$	0
10^{-3}	150	$0,15 \times L$	0
10^{-4}	450	$0,45 \times L$	0

Waveform 3: 25/1 500 µs.
Source impedance: $Z_s = 50\ \Omega$.

5.4 Late-time HEMP external conducted environment

The late-time HEMP environment is only important for coupling to long external conductors such as power and communication lines. In this case, however, the computation of short-circuit currents for typical cases of interest is not easily accomplished. This is because the late-time HEMP environment is described as a voltage source that is produced in the earth which induces currents to flow only in conductors that are connected to the earth at two or more points. Since the current that flows is strongly dependent on the resistance present in the circuit, an analytical method is provided here to develop a standard conducted environment.

In order to describe the method to be used, an example case is provided. In Figure 4a), a three-phase Y-delta power configuration is shown along with an equivalent circuit in Figure 4b) (where E_0 is the peak value of the late-time HEMP). Note that the problem can be described as a quasi-DC problem with the voltage source calculated directly from the late-time HEMP environment. Since the highest frequencies contained in the late-time HEMP environment are of the order of 1 Hz, this is clearly appropriate. It can therefore be assumed that the voltage source V_s has the same time dependence as E_0 . Given that the resistances shown in the lower portion of Figure 4 (the parallel Y winding resistances R_y and the "footing" or grounding resistances R_f) are not frequency dependent for $f < 1$ Hz, then the induced current I_{pk} will have the same time dependence as E_0 .

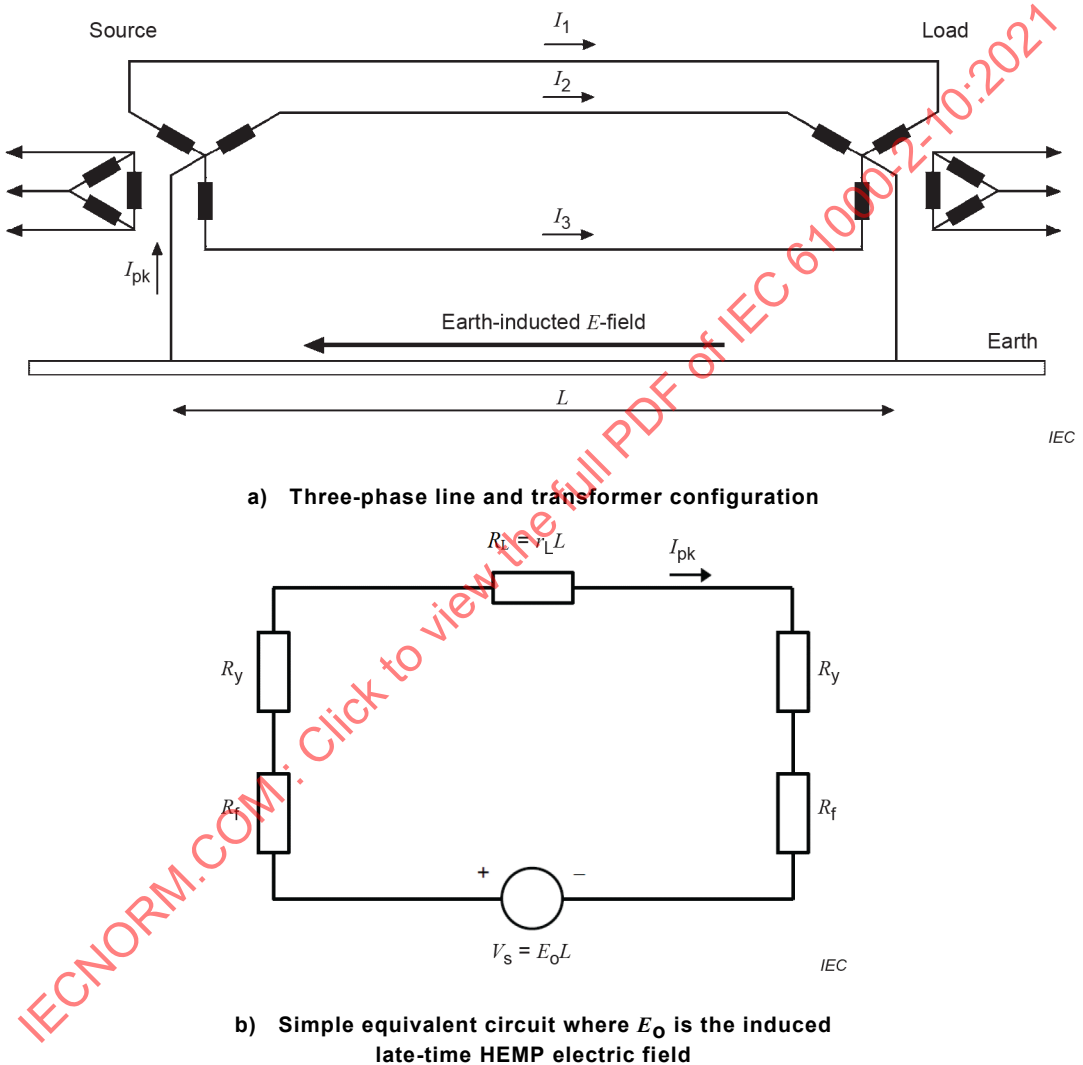


Figure 4 – Three-phase line and equivalent circuit for computing late-time HEMP conducted current

Using the example provided, the peak current can be calculated as:

$$I_{pk} = \frac{E_0 L}{2(R_f + R_y) + r_L L} \quad (1)$$

where

r_L is the parallel wire resistance per unit length (Ω/m);

R_f is the ground resistance (Ω);

R_y is the parallel winding resistance in one transformer (Ω);

L is the line length (m).

For a long transmission line in North America, a 500 kV line would have a resistance per unit length of $8,3 \times 10^{-6} \Omega/m$, a transformer winding resistance of $0,06 \Omega$ and a grounding resistance of $0,75 \Omega$. For a 10^5 m length line and a peak field E_0 of $0,04 \text{ V/m}$ (from IEC 61000-2-9), this formula results in a peak current of approximately 1 630 A. Given this peak value, the current time waveform can be approximated by a unipolar pulse with a rise time and pulse width of 1/50 s. To simulate the waveform for this example, one could use a voltage source of 4 kV with a source impedance of $2,45 \Omega$. It is important to recognize the necessity to ground transformers in order to use the circuit in Figure 4. Some transformers are delta-delta and do not possess a direct path to ground as shown in the figure.

Formula (1) above can easily be translated to cover cases other than power lines by computing the total resistance in the circuit, and dividing it into the total voltage induced over the length of the conductor. Formula (1) is provided for the case of long cables overland, and for deep undersea cables the currents calculated may be reduced by up to a factor of 100. This reduction is due to the behaviour of the electric field E_0 which is inversely proportional to the square root of the deep ground conductivity (to depths of 10 km to 100 km). For freshwater lakes or shallow seas, the currents may not be reduced as much.

5.5 Antenna currents

Antennas come in many different sizes and shapes. At frequencies in the VLF and LF range (3 kHz to 300 kHz), such antennas are often in the form of very long wires which are sometimes buried in the earth. Antennas in the MF band (300 kHz to 3 000 kHz) are often in the form of a vertical tower which is fed against a buried counterpoise grid buried in the earth. In the HF and VHF bands (3 MHz to 30 MHz and 30 MHz to 300 MHz, respectively), the antennas typically appear as centre-fed dipoles, and at the higher frequencies (UHF, SHF, etc.) they become more like a distributed system, involving reflecting dishes and radiating apertures.

Usually, antennas are operated in a narrow band of frequencies located around a fundamental design frequency. In order to enhance their narrow-band performance, such antennas are often "tuned" by adding lumped impedance elements, by adding additional passive elements near the active antenna, or by locating the antenna in an array.

Given such a large variation in antenna configurations, it is difficult to provide an accurate response specification (current and voltage waveforms) for every type of antenna. As an approximate model, however, it is possible to consider the simple thin-wire vertical dipole antenna shown in Figure 5, and to use its response as an indication of what would be the responses for other more complex antennas. Of course, this model is applicable only to antennas of the electric dipole class: loop (i.e., magnetic) antennas and aperture antennas are not adequately modelled by this simple structure. For more complex antennas, it is recommended that CW illumination or high-level pulse testing be performed to evaluate antenna responses.

These types of test methods are described in IEC 61000-4-23.

The antenna in Figure 5 is assumed to be loaded by a nominal 50Ω resistance, which is typical of a realistic in-band load on the antenna. The antenna has an end-to-end length of l and a radius of a ; these parameters are used to compute the form parameter $\Omega = 2 \ln(l/a)$. The resonance bandwidth factor Q (which also defines the damping factor of a sinusoid in the time domain) of the load current of this antenna may be approximated by $Q = \Omega/3,6$. For non-ideal antennas, the Q parameter should be derived from antenna response measurements.

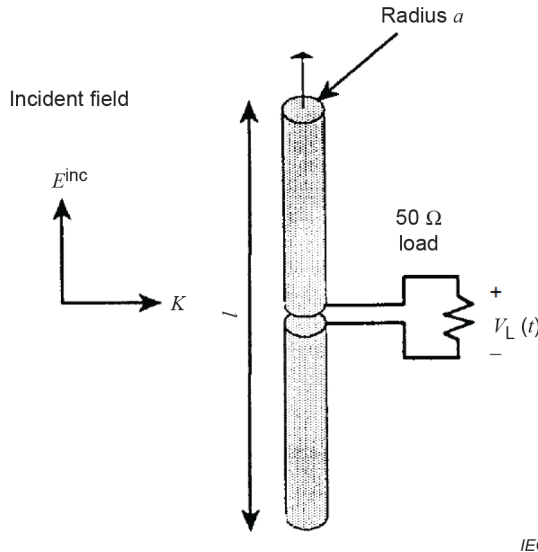


Figure 5 – Centre-loaded dipole antenna of length l and radius a , excited by an incident early-time HEMP field

Usually, the antenna of Figure 5 is located in the vicinity of other conducting bodies that modify the incident field and, consequently, change the response from that obtained for the isolated antenna. For example, the antenna can be located on or near the ground where an earth-reflected field can provide an additional antenna excitation. Equally the dipole might be mounted on a long mast where the scattered field from the mast and support wires will modify the excitation.

As with the variations in the antenna geometry, it is difficult to take into account all of these possibilities in developing a standard response waveform. The problem is made a bit easier, however, by the fact that in many cases, the reflected field arrives at the antenna after the incident field has excited the antenna, suggesting that the incident field response can still provide an adequate specification of the response. For this simplified specification process, the influence of any scattered field excitation is neglected.

To calculate the response of the antenna, the fundamental resonance frequency is given by

$$f_c = \frac{c}{2l} \quad (2)$$

where

c is the speed of light, and

l is the total length of a dipole or twice the height of a monopole over a ground plane.

The response of the antenna is then given as a load current into 50Ω :

$$I_L(t) = k I_p e^{\frac{-\pi f_c t}{Q}} \sin(2\pi f_c t) \text{ for } t \geq 0 \quad (3)$$

with I_p defined in Table 3. The normalizing factor k is defined to allow I_L to peak at a value of I_p , and it depends on the values of Q and f_c . In Table 3, I_p is defined as the product $I H_p$, where H_p is the peak incident HEMP magnetic field. Below 10 MHz the peak antenna current is assumed constant.

Table 3 – Maximum peak electric dipole antenna load current versus frequency for antenna principal frequencies

(MHz)	<i>l</i> (m)	<i>H_p</i> (A/m)	<i>lH_p</i> (A)	<i>I_p</i> (A)
< 1	> 150	—	—	2 000 ^a
1 to 10	15 to 150	—	—	2 000 ^a
10	15	130	1 950	1 950
100	1,5	130	195	195
200	0,75	130	97,5	97,5
> 200	150/fc	130	19 500/fc	19 500/f _c

While the previous approach provides near-worst case coupling results for a thin-wire vertical dipole antenna (but without earth reflections), it is possible to provide probabilistic coupling information using a technique similar to that employed earlier in Table 1. Using an approach which considers the variation of the angle of elevation with area coverage from a 100 km burst height, Annex C provides detailed coupling results for two thin wire antennas. These include a vertical monopole antenna of length l_m (including HEMP earth reflections) and a horizontal dipole antenna of length l_h (without earth reflections), both with 50Ω loads. These peak results are summarized in Table 4 to Table 6 for the vertical monopole antenna and Table 7 to Table 9 for the horizontal dipole. Annex E provides a procedure for determining the time waveform description for analysis and testing.

Table 4 – HEMP response levels for V_{oc} for the vertical monopole antenna

Table 5 – HEMP response levels for I_{sc} for the vertical monopole antenna

Values are in kA												
Length l_m	1 m			3 m			10 m			100 m		
Severity	50 %	90 %	99 %	50 %	90 %	99 %	50 %	90 %	99 %	50 %	90 %	99 %
Dip angle												
0°	0,08	0,19	0,22	0,33	0,66	0,70	1,12	1,74	1,91	3,13	3,68	4,37
15°	0,08	0,18	0,21	0,32	0,64	0,68	1,13	1,68	1,85	3,02	3,55	4,31
30°	0,07	0,16	0,19	0,28	0,57	0,61	0,96	1,50	1,65	2,71	3,25	4,13
45°	0,06	0,13	0,16	0,23	0,47	0,50	0,79	1,23	1,35	2,23	2,72	3,67
60°	0,04	0,10	0,11	0,16	0,33	0,35	0,57	0,87	0,95	1,57	1,94	2,73
75°	0,02	0,05	0,06	0,08	0,17	0,18	0,30	0,45	0,49	0,81	1,01	1,38
90°	0	0	0	0	0	0	0	0	0	0	0	0

Table 6 – HEMP response levels for I_L for the loaded vertical monopole antenna^a

Values are in kA												
Length l_m	1 m			3 m			10 m			100 m		
Severity	50 %	90 %	99 %	50 %	90 %	99 %	50 %	90 %	99 %	50 %	90 %	99 %
Dip angle												
0°	0,06	0,15	0,17	0,23	0,49	0,55	0,76	1,31	1,33	2,37	2,71	3,53
15°	0,06	0,14	0,16	0,23	0,48	0,53	0,76	1,26	1,29	2,28	2,59	3,34
30°	0,05	0,13	0,15	0,20	0,43	0,47	0,65	1,13	1,15	2,03	2,32	3,00
45°	0,04	0,10	0,12	0,16	0,35	0,39	0,54	0,92	0,94	1,69	1,91	2,51
60°	0,03	0,07	0,08	0,12	0,25	0,27	0,39	0,65	0,67	1,17	1,35	1,79
75°	0,02	0,04	0,04	0,06	0,13	0,14	0,20	0,34	0,34	0,61	0,70	0,91
90°	0	0	0	0	0	0	0	0	0	0	0	0

^a For the corresponding load voltage values, multiply these values by 50 Ω.

Table 7 – HEMP response levels for V_{oc} for the horizontal dipole antenna

Values are in kV												
Length l_h	1 m			3 m			10 m			100 m		
Severity	50 %	90 %	99 %	50 %	90 %	99 %	50 %	90 %	99 %	50 %	90 %	99 %
Dip angle												
0°	0,8	4,0	11,5	2,8	13,5	44,0	7,9	37,9	110,4	19,0	99,8	289,1
15°	4,9	7,0	13,1	17,1	25,1	45,8	44,3	68,2	113,3	115,3	162,2	309,1
30°	8,9	12,5	15,4	31,0	45,6	53,9	81,3	128,1	154,6	211,9	291,0	367,3
45°	12,5	17,6	18,6	43,1	64,1	67,3	112,7	179,7	188,2	293,9	407,4	434,7
60°	15,1	21,4	21,9	52,5	78,2	79,8	136,2	218,6	224,0	355,4	495,9	508,0
75°	16,8	23,9	24,2	58,3	87,0	88,4	152,2	243,9	248,6	395,1	552,1	563,6
90°	18,0	24,6	25,1	60,0	89,9	91,5	159,4	251,7	257,2	404,8	573,1	583,3

Table 8 – HEMP response levels for I_{sc} for the horizontal dipole antenna

Values are in kA												
Length l_h	1 m			3 m			10 m			100 m		
Severity	50 %	90 %	99 %	50 %	90 %	99 %	50 %	90 %	99 %	50 %	90 %	99 %
Dip angle												
0°	0,003	0,01	0,04	0,01	0,05	0,15	0,03	0,16	0,47	0,10	0,53	1,66
15°	0,02	0,02	0,04	0,06	0,09	0,17	0,19	0,27	0,48	0,55	0,81	1,71
30°	0,03	0,04	0,05	0,11	0,17	0,20	0,35	0,49	0,62	1,04	1,36	1,99
45°	0,04	0,06	0,06	0,15	0,24	0,25	0,49	0,69	0,73	1,47	1,87	2,27
60°	0,05	0,07	0,07	0,18	0,29	0,30	0,59	0,84	0,86	1,79	2,27	2,52
75°	0,05	0,08	0,08	0,20	0,32	0,33	0,65	0,94	0,96	2,00	2,52	2,65
90°	0,05	0,08	0,08	0,21	0,34	0,34	0,67	0,97	0,99	2,06	2,61	2,69

Table 9 – HEMP response levels for I_L for the loaded horizontal dipole antenna^a

Values are in kA												
Length l_h	1 m			3 m			10 m			100 m		
Severity	50 %	90 %	99 %	50 %	90 %	99 %	50 %	90 %	99 %	50 %	90 %	99 %
Dip angle												
0°	0,002	0,012	0,032	0,008	0,040	0,13	0,028	0,14	0,39	0,078	0,42	1,26
15°	0,014	0,020	0,036	0,050	0,078	0,14	0,16	0,23	0,40	0,45	0,65	1,33
30°	0,024	0,036	0,044	0,092	0,15	0,17	0,29	0,44	0,54	0,84	1,10	1,58
45°	0,034	0,050	0,054	0,13	0,20	0,22	0,41	0,61	0,64	1,17	1,51	1,83
60°	0,042	0,062	0,062	0,16	0,25	0,26	0,50	0,74	0,76	1,44	1,83	2,05
75°	0,046	0,068	0,070	0,17	0,28	0,29	0,55	0,83	0,85	1,60	2,04	2,18
90°	0,048	0,070	0,072	0,17	0,28	0,30	0,57	0,86	0,88	1,66	2,10	2,22

^a For the corresponding load voltage values, multiply these values by 50 Ω.

5.6 HEMP internal conducted environments

As discussed previously, the internal conducted environments (inside of a building or installation) are more difficult to determine than the external conducted environments. The internal conducted signals are produced by external conducted signals which penetrate through a shield (with or without attenuation due to PoE hardening), and by any HEMP fields which are able to penetrate the building and couple to exposed wiring. Because there is a large variety of electromagnetic shield materials for buildings which range from wood construction to high-quality welded steel shield rooms, it is difficult to calculate the coupling to cables and other conductors inside a facility. It is, however, possible to define a simple procedure which will allow one to estimate the internal conducted transients.

The first step in the internal conductor problem is to recognize that the leakage of external conducted transients is a major consideration. One should take the conducted environments specified above and determine the type of protection present at the entry point into the facility. Using either analyses or test data, one can estimate the current waveform that penetrates the facility. It should be noted that if a non-linear device is present, it will probably be necessary to perform a test using IEC 61000-4-24, unless the amount of suppression is expected to be very high.

The second step is to estimate the amount of electromagnetic attenuation that will occur for the early-time HEMP radiated environment. (It is not necessary to evaluate the intermediate or late-time field attenuation because those low frequency fields will not couple well to the compact cable geometries present inside most facilities.) Defining A_t as the plane wave attenuation factor (for $f > 1$ MHz), D as the internal cable length of interest in metres, and B as an amplitude factor based on the severity factors introduced in Table 1, one can estimate the peak internal common mode cable current I_{pk} as

$$I_{pk} = BDA_t \text{ for } D < 100 \text{ m} \quad (4)$$

The amplitude parameter B in units of A/m has been developed so the product BD is consistent with the last column in Table 1, elevated conductor; B is defined as 5,0 A/m, 7,5 A/m and 20 A/m for severity levels of 50 %, 90 % and 99 %, respectively. Therefore, for a severity level of 50 %, a building attenuation factor of 0,01 (–40 dB) and a conductor length of 10 m, the peak coupled current is 0,5 A. As indicated in Annex D, the current waveforms produced are expected to resemble damped sinusoids. Formulae (2) and (3) should be employed assuming $l = D$ and $Q \geq 60$.

This process is not precise because the attenuation of an incident electromagnetic field is not uniform with frequency, especially if apertures are present. In addition, once the internal field is established, there are often many cables present that make accurate coupling calculations difficult. Finally, the size and shape of a facility will produce cavity modes that will impact the waveshape of the coupled currents. In spite of these difficulties, this procedure can provide a rough estimate of the internal conducted currents.

A second alternative procedure for estimating internal conducted currents I_{pk} due to HEMP includes the direct use of data collected in the past for three classes of building construction. As provided in Annex D, the 50 %, 90 %, and 99 % severity currents are given for concrete block, riveted metal and poured concrete construction. 50 % peak-to-peak currents are 10 A, 10 A and 3 A for the three construction methods, while the 99 % values are 25 A, 25 A and 7 A, respectively. These internal currents are due to external HEMP field coupling only and do not include the contribution of currents which enter through penetrating conductors. The time waveforms of the currents are found using Formulae (2) and (3), with $f_c = 7$ MHz and $Q \geq 60$.

A third (and most accurate) procedure for deriving the internal conductor currents is through experimental measurements. The procedure usually involves the use of a continuous wave simulator over the range of 100 kHz to 500 MHz. The building is exposed at several positions for different angles of elevation and field polarizations while measuring the internal cable currents. The transfer functions are then convolved with the incident early-time HEMP waveform to compute internal cable current waveforms. It is usually necessary to evaluate the variation of the current waveform peak values and pulse shapes to develop composite waveforms for equipment testing purposes.

It is important to recognize that the three procedures indicated here provide only the internal currents due to direct HEMP field coupling. It is necessary to estimate (or measure) the leakage of external currents through the facility walls (including surge protection) to determine the contribution of the external currents to the total internal currents.

Annex A

(informative)

Discussion of early-time HEMP coupling for long lines

A.1 Elevated line coupling

The results presented earlier in Table 1 were produced from a series of probabilistic coupling calculations from Ianoz et al [1]¹. In these calculations, the authors used the IEC early-time HEMP electric field pulse as defined in IEC 61000-2-9 to compute the coupling (short-circuit current) to a 10 m high, 1 km long line over a ground with a 10^{-2} S/m conductivity. The calculations were performed separately for both 100 % horizontal and 100 % vertical polarization. For each polarization, angles of elevation ψ and azimuth ϕ between the incident field propagation vector and the line were varied over a 2,5° mesh. These results were saved and recombined for any burst height and earth location (by the geomagnetic latitude) of interest.

Figure A.1 presents a summary of the calculations for a 100 km burst for five magnetic dip angles (0° , 45° , 67° , 75° and 90°). For the coupling results, the 0° results were not used here because the coupling calculations did not consider the reduction of the HEMP electric field due to the lower value of earth's magnetic field at the magnetic equator. This would result in a reduction of the incident field and the coupled currents by 30 % to 40 %. From the results shown ($\theta_{\text{dip}} > 45^\circ$) in Figure A.1, the selection of 4 000 A for 1,0 % of the cases, 1 500 A for 10 %, and 500 A for 50 % is indicated (within 10 % accuracy). The 1 %, 10 %, and 50 % probabilities discussed in Annex A are equivalent to the 99 %, 90 % and 50 % severity levels discussed in Clause 5.

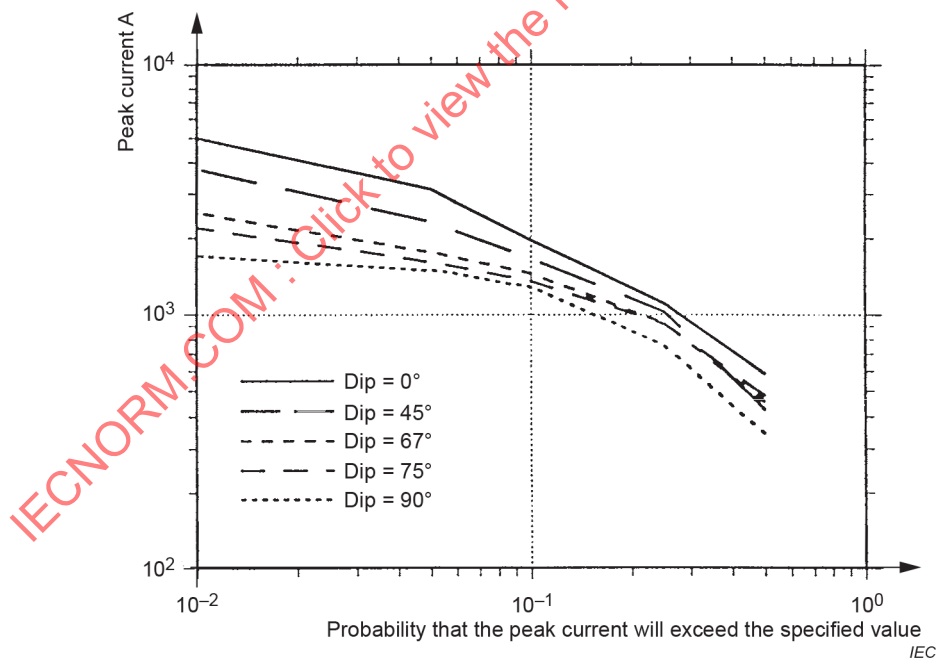


Figure A.1 – Variation of peak coupled cable current versus local geomagnetic dip angle

¹ Numbers in square brackets refer to the Bibliography.

For the time waveform current characteristics presented in this document, the study performed in [1] also considered several waveform characteristics including the waveform rise time (10 % to 90 %) and the rectified impulse which is the pulse area for a monopolar pulse. The rectified impulse values for the vertical polarizations are given in Table A.1 along with the computation of the effective pulse width, Δt_{pw} (rectified impulse divided by peak), using the specified peak currents.

Table A.1 – Rectified impulse (RI) and computed effective pulse widths for vertical polarization of the early-time HEMP for an elevated conductor ($h = 10$ m)

Probability	$RI >$	Peak $I >$	Δt_{pw}
%	$A \times s$	A	ns
50	$3,7 \times 10^{-5}$	500	74
10	$1,9 \times 10^{-4}$	1 500	127
1	$3,0 \times 10^{-4}$	4 000	75

For this evaluation a maximum effective pulse width of 127 ns is selected and is translated into a pulse width at half maximum of 88 ns by assuming an exponentially decaying waveform. This is approximated as 100 ns in Table 1.

The evaluation of the rise time characteristics was more difficult for this coupling study. The 10 % to 90 % rise time was tabulated in [1] for both horizontal and vertical HEMP polarization. The results indicated minimum rise times of 2,3 ns and 5,1 ns for horizontal and vertical field polarization. After careful examination it was found that these rise times did not occur when the peak currents were the largest. Since the derivative itself was not tabulated in that study, additional calculations were required.

For complete vertical polarization of the IEC electric field pulse, a maximum current derivative of $2,7 \times 10^{11}$ A/s was calculated at an elevation angle of 5° for the same coupling geometry used in [1]. This maximum value was found from a series of calculations, and the peak value of the coupled current was maximized at the same angle. For the specified 1 % probability case, the computed 10 % to 90 % rise time is:

$$(0,8) \times (4 000 \text{ A}) / (2,7 \times 10^{11} \text{ A/s}) = 1,2 \times 10^{-8} \text{ s}$$

For the purposes of this document, a rise time of 10 ns was selected. Although it appeared likely that slower rise times would be appropriate for the more probable cases, calculations showed that the 50 % case indicated a rise time of 14,4 ns. Therefore, given the relatively small difference, the same pulse rise time is used for all cases in Table 1.

A.2 Buried line coupling

For buried communications or power lines, the coupled HEMP signal does not vary substantially with field polarization or angle, although the near-surface ground conductivity is of some importance. HEMP calculations using the IEC pulse were performed for a line buried at a depth of 1,0 m in three ground conductivities: 10^{-2} S/m, 10^{-3} S/m and 10^{-4} S/m. The results of 42 calculations which considered variations in angles of elevations and field polarization are summarized in Table A.2.

Table A.2 – Coupled early-time HEMP currents for a buried conductor ($z = -1$ m)

σ_g S/m	Polarization	Max I_{sc} A	ψ degrees
10^{-2}	V	152	60
10^{-2}	H	148	90
10^{-3}	V	332	45
10^{-3}	H	267	90
10^{-4}	V	437	30
10^{-4}	H	418	90

For the two lower conductivities, these values are rounded to the nearest 100 A in Table 1 ($10^{-3} – 300$ A, $10^{-4} – 400$ A) which creates in both cases a 10 % reduction. For the higher conducting ground entries shown in Table A.2, the current is adjusted upward to 200 A to account for the higher field levels nearer to the earth's surface (appropriate for shallower burial depths).

In terms of the waveshapes to be used, the range of 10 % to 90 % rise times and pulse widths at half maximum are given in Table A.3.

Table A.3 – Waveform parameters for early-time HEMP buried conductor coupling ($z = -1$ m)

σ_g S/m	Polarization	Δt_r (10 % to 90 %) ns	Δt_{pw} (50 % to 50 %) ns
10^{-2}	V	26,7 to 34,7	185 to 355
10^{-2}	H	17,6 to 19,5	263 to 282
10^{-3}	V	25,0 to 29,2	198 to 398
10^{-3}	H	19,3 to 26,5	236 to 267
10^{-4}	V	27,0 to 29,8	309 to 583
10^{-4}	H	27,4 to 29,3	361 to 458

Averaging the variations provided in Table A.3 for each ground conductivity, Table A.4 indicates the results.

Table A.4 –Average waveform parameters for early-time HEMP buried conductor currents

σ_g S/m	Δt_r (10 % to 90 %) ns	Δt_{pw} (50 % to 50 %) ns
10^{-2}	24,6	271
10^{-3}	25,0	275
10^{-4}	28,4	428

Given this information, it is recommended that a rise time of 25 ns be used. For the pulse width, the variations are stronger with ground conductivity, and a value of 500 ns is recommended (rather than 400 ns) to cover the larger pulse widths computed (see Table A.3) for low ground conductivity. These values are applied in Table 1.

Annex B

(informative)

Discussion of intermediate-time HEMP coupling for long lines

B.1 General

The short-circuit results presented in Table 2 were produced from a series of 70 HEMP coupling calculations for an elevated ($h = 10$ m) and buried ($h = -1$ m) conductor. The study considered variations in line length (1 km to 100 km), angle of elevation (0° to 85°) and ground conductivity (10^{-2} S/m, 10^{-3} S/m and 10^{-4} S/m). A time-dependent transmission line code was employed for the calculations, and the IEC incident intermediate-time waveform was used assuming vertical polarization.

B.2 Elevated line coupling

For lines greater than 10 km in length, the maximum peak short-circuit currents and waveform characteristics are shown in Table B.1.

Table B.1 – Coupled HEMP intermediate-time short-circuit currents for an elevated conductor ($h = 10$ m)

Ground conductivity S/m	I_{pk} A	Δt_r (10 % to 90 %) μs	Δt_{pw} μs
10^{-2}	138	60 to 120	700 to 2 100
10^{-3}	342	25 to 65	850 to 2 100
10^{-4}	849	30 to 65	1 000 to 2 100

For shorter lines, the peak currents are reduced but the pulse characteristics are similar. Recommended values for the peak currents are approximated as 150 A, 350 A and 850 A in Table 2. The pulse characteristics can be approximated to provide a rise time of 25 μs and an effective pulse width of 2 100 μs; this effective pulse width is converted to a pulse width at half maximum of 1 500 μs.

B.3 Buried line coupling

For buried lines longer than 1 km, the peak currents calculated are nearly constant, varying only with the ground conductivity. For line lengths shorter than 1 km, length scaling is appropriate. Angle of incidence variations for elevation angles from 0° to 85° indicate a variation of less than 10 %. Table B.2 presents the summary of the HEMP calculations.

Table B.2 – Coupled HEMP intermediate-time short-circuit currents for a buried conductor ($h = -1$ m)

Ground conductivity S/m	I_{pk} A	Δt_r (10 % to 90 %) μs	Δt_{pw} μs
10^{-2}	46	38 to 57	1 800 to 2 000
10^{-3}	147	40 to 61	1 900 to 2 100
10^{-4}	431	46 to 78	1 900 to 2 100

The results shown above can be approximated for peak values of 50 A, 150 A and 450 A by a single pulse waveform with a rise time (10 % to 90 %) of 40 μ s and an effective pulse width of 2 100 μ s. Converting the effective pulse width to a half width (assuming an exponential decay) yields a value of 1 455 μ s or 1 500 μ s. Because the waveform characteristics are similar for both elevated and buried lines, only a single waveform is required in Table 2, and the values of 25 μ s and 1 500 μ s are used.

IECNORM.COM : Click to view the full PDF of IEC 61000-2-10:2021

Annex C

(informative)

Responses of simple linear antennas to the IEC early-time HEMP environment

C.1 Overview

For the understanding of the protection requirements of civilian systems against the effects of a high-altitude electromagnetic pulse (HEMP), it is useful to have an indication of the possible responses of various types of antennas. The analysis of antennas is a mature discipline, with many different calculational models available for use in determining typical responses [2]. However, the analysis of antennas is frequently conducted only in the in-band (i.e., the operational) frequency range, and this is not particularly useful for obtaining the transient response of an antenna, in which a very wide-band analysis is required.

Furthermore, when a transient response of an antenna is conducted, the results are often presented in the form of a transient waveform for a limited number of angles of incidence of the excitation. Thus, a global understanding of the behaviour of the antenna and its typical responses usually is not available.

One way of remedying this situation is to perform a large number of individual transient antenna calculations for different angles of incidence of the HEMP and then to present the results of the antenna response (e.g., the peak value of the open-circuit voltage of the antenna) in the form of a cumulative probability distribution (CPD) which provides an indication of the probability of a response of the antenna exceeding a specified value. In this document, the responses of two different antennas are determined for the IEC early-time HEMP environment. The antennas are a vertical monopole antenna which is assumed to be fed against the earth, and a horizontal dipole antenna which is located above the earth. In each of these cases, the observables considered are the peak values of the open-circuit voltage (V_{oc}), the short-circuit current (I_{sc}), the peak voltage across a $50\ \Omega$ load connected to the input of the antenna (V_L), and the corresponding peak current flowing through the $50\ \Omega$ load (I_L).

C.2 IEC early-time HEMP environment

As described in IEC 61000-2-9, the HEMP is represented by an incident plane wave shown in Figure C.1 which is incident on a system on or near the ground with a vertical angle of elevation ψ and an azimuthal angle of incidence ϕ , which is measured with respect to some convenient reference direction (the x -axis).

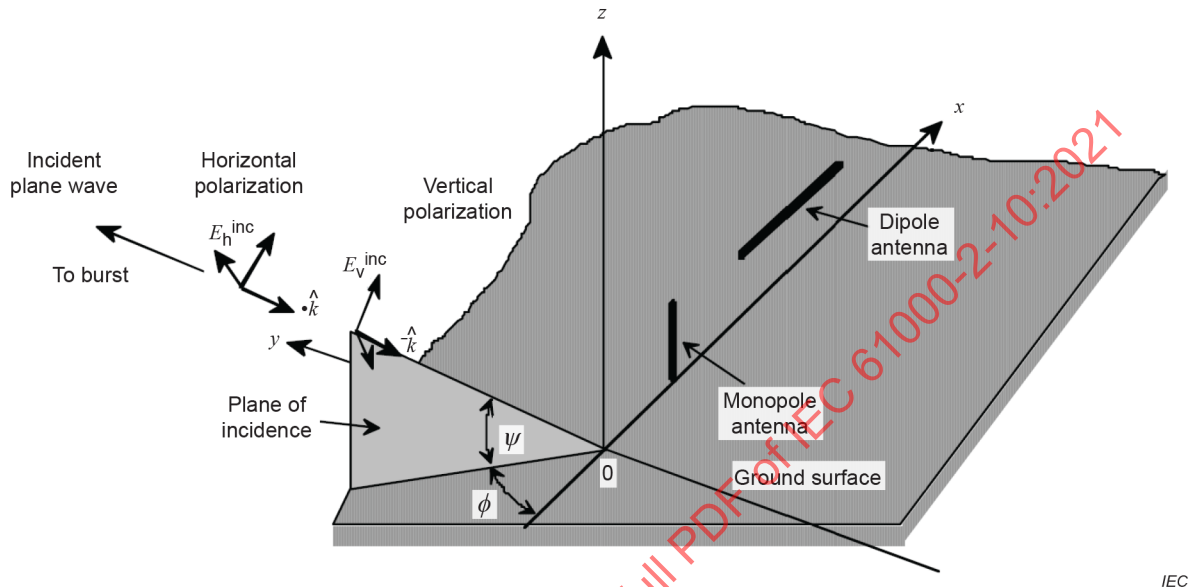
Because of the spherical earth geometry, only a limited area on the earth's surface is directly illuminated by the HEMP fields. As shown in Figure C.2, the illuminated region on the earth is defined by the tangent radius R_t in km, which is given by the expression

$$R_t = R_e \arccos\left(\frac{R_e}{R_e + HOB}\right) \quad (C.1)$$

where HOB is the height of the burst in km, and R_e is the earth radius (6 371,2 km). For $HOB < 500$ km, this expression is approximated by

$$R_t \approx 110 \sqrt{HOB \times 1 \text{ km}} \quad (\text{C.2})$$

For the present study, it is assumed that the burst is located at a height of 100 km. This implies that the tangent radius is $R_t \approx 1100 \text{ km}$.



IEC

Figure C.1 – Illustration of the incident HEMP field

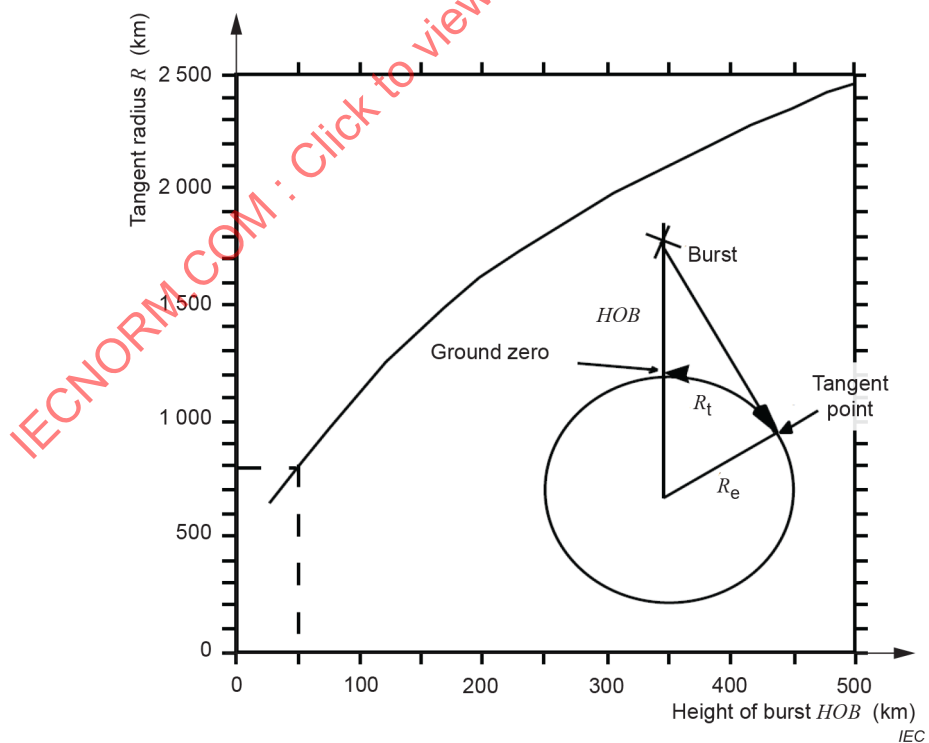


Figure C.2 – HEMP tangent radius R_t defining the illuminated region, shown as a function of burst height (HOB)

Outside the illuminated region, the HEMP fields are taken to be zero. Within this region, the incident field is assumed to have a time history given by a double exponential waveform of the form

$$E^{\text{inc}}(t) = 65000 \left(e^{-4 \times 10^7 t} - e^{-6 \times 10^8 t} \right) \quad t > 0 \quad (\text{C.3})$$

where E is in units of V/m and t is in units of seconds. The linearly polarized waveform is decomposed into vertically and horizontally polarized components, as indicated in Figure C.1.

As discussed in IEC 61000-2-9, the division of the incident HEMP field into vertical and horizontal components depends on the dip angle of the geomagnetic field θ_{dip} . This parameter varies with the locations of the burst and observer, and hence, it is treated as an independent variable in this study: responses for different values of θ_{dip} are calculated. The vertical and horizontal components of the incident field are denoted by E_v^{inc} and E_h^{inc} and are given in terms of the polarization fractions f_v and f_h , as $E_v^{\text{inc}} = f_v E^{\text{inc}}$ and $E_h^{\text{inc}} = f_h E^{\text{inc}}$. For this study the polarization fractions have been approximated at their maximum values, $f_v = \cos \theta_{\text{dip}}$ and $f_h = \sin \theta_{\text{dip}}$.

As shown in Figure C.1, the two antennas considered are a vertical monopole antenna mounted on the earth, and a horizontal dipole antenna extended parallel to the earth. To compute the induced current in these antennas, it is necessary to know the tangential excitation E -field along the antennas. This field consists of the incident HEMP field, plus the ground-reflected field. For the vertical monopole, the excitation field is the z -component of the E -field, which at any height z , is given as [3]:

$$E_z = E^{\text{inc}} \cos \theta_{\text{dip}} \cos \psi \left(1 - R_v e^{-jk2z \sin \psi} \right) \quad (\text{C.4})$$

where E is in units of V/m, k is in units of 1/m and z is given in metres. R_v is the Fresnel reflection coefficient for a vertically polarized field, given by [4]:

$$R_v = \frac{\varepsilon_r \left(1 + \frac{\sigma_g}{jw\varepsilon_r\varepsilon_0} \right) \sin \psi - \left[\varepsilon_r \left(1 + \frac{\sigma_g}{jw\varepsilon_r\varepsilon_0} - \cos^2 \psi \right) \right]^{1/2}}{\varepsilon_r \left(1 + \frac{\sigma_g}{jw\varepsilon_r\varepsilon_0} \right) \sin \psi + \left[\varepsilon_r \left(1 + \frac{\sigma_g}{jw\varepsilon_r\varepsilon_0} - \cos^2 \psi \right) \right]^{1/2}} \quad (\text{C.5})$$

where σ_g is the electrical conductivity of the ground, ε_r is the relative permittivity of the ground and ε_0 is the free-space permittivity. Notice that for this vertical field, only the vertically polarized component of the incident HEMP field contributes to the response.

For the horizontal antenna, which is assumed to be parallel to the x -axis, the E_x field component at a height h over the ground is required as the excitation. This field is expressed in terms of both the vertically polarized and horizontally polarized waveform components as [3]:

$$E_x = E^{\text{inc}} e^{-jkx \cos\psi \cos\phi} \left[\cos\theta_{\text{dip}} \sin\psi \cos\phi \left(1 - R_v e^{jk2h \sin\psi} \right) + \sin\theta_{\text{dip}} \sin\phi \left(1 + R_v e^{jk2h \sin\psi} \right) \right] \quad (\text{C.6})$$

where the Fresnel reflection for the horizontal field, R_h , has been introduced. This is also given in [4] as

$$R_h = \frac{\sin\psi - \left[\varepsilon_r \left(1 + \frac{\sigma_g}{j\omega \varepsilon_r \varepsilon_0} \right) - \cos^2\psi \right]^{1/2}}{\sin\psi + \left[\varepsilon_r \left(1 + \frac{\sigma_g}{j\omega \varepsilon_r \varepsilon_0} \right) - \cos^2\psi \right]^{1/2}} \quad (\text{C.7})$$

C.3 Evaluation of the antenna responses

C.3.1 General

Given the tangential excitation fields of Formula (C.4) and Formula (C.6), together with a specification of the antenna length, radius and load impedance, the induced currents on a given antenna and in the loads can be computed by using the method of moments [5]. This is a numerical procedure which solves the frequency-dependent integral formula for the current. Once the frequency domain spectrum of the response is computed, the transient response is computed using the fast Fourier transform (FFT). Details of such calculations are presented in [6] and [7].

C.3.2 Monopole antenna

Figure C.3 illustrates the geometry of the vertical monopole used in this study. As noted in Formula (C.4), the excitation field is independent of the azimuthal angle ϕ . Consequently, only the vertical angle of elevation ψ enters into the calculation. The monopole has a length L , a radius a , and has a 50Ω load at the base of the antenna connected to the ground. For such antennas, it is common to specify the length to radius ratio through a parameter Ω_0 , defined as

$$\Omega_0 = 2 \ln \left(\frac{2L}{a} \right) \quad (\text{C.8})$$

For the present calculation, the parameter $\Omega_0 = 8$, which corresponds to an L/a ratio of 27,3, represents a reasonably thick antenna.

In these calculations, the earth is taken to have a conductivity $\sigma_g = 0,01 \text{ S/m}$ and a relative permittivity $\varepsilon_r = 10$, which are typical values according to [4].

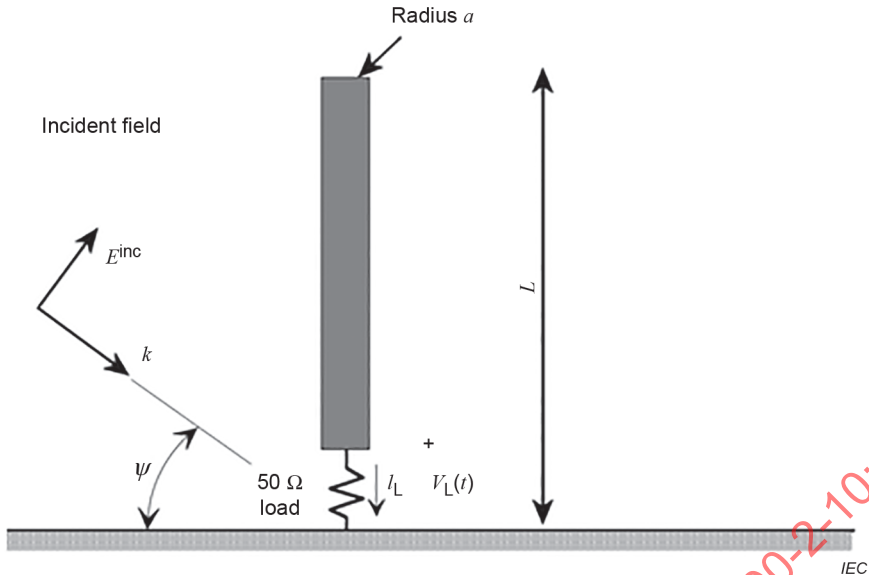


Figure C.3 – Geometry of the monopole antenna

For this antenna (as well as for the dipole to be discussed in C.3.3, four quantities have been calculated: the open-circuit voltage (V_{oc}) at the source "gap" located at the base of the antenna, the short-circuit current (I_{sc}) flowing at the base of the antenna, the loaded voltage (V_L) across the impedance at the input of the antenna, and the corresponding load current (I_L). All of these quantities are related by the integral formula for the antenna current as described by Harrington [5]. Because of the simple V - I relationship at the load impedance, the load voltage and load current are related trivially by $V_L = Z_L I_L$. Of special interest here is the peak value of the transient responses, and these are the quantities actually extracted and retained as the calculation progresses.

The determination of the CPDs for the above observables involves performing a large number of calculations of the antenna responses as an observation point is chosen at random in the illumination region. Typically, 3 000 distinct observation locations have been used and for each location, the solution of the integral formula is used to provide a knowledge of the observable values. This leads to a distribution of responses and ultimately to the CPD, which provides the probability of a particular response exceeding a specified value.

C.3.3 Dipole antenna

The geometry of the horizontal dipole antenna is shown in Figure C.4. The excitation function for this antenna depends on both the ϕ and ψ angles of incidence, as well as on both polarization components of the incident field. For this antenna, the total length is denoted by L , the radius is a , and the load impedance is again chosen to be 50Ω . The length to radius ratio for this case is defined as

$$\Omega_0 = 2 \ln \left(\frac{L}{a} \right) \quad (C.9)$$

where again the parameter $\Omega_0 = 8$ has been used. This corresponds to an L/a ratio of 54,6.

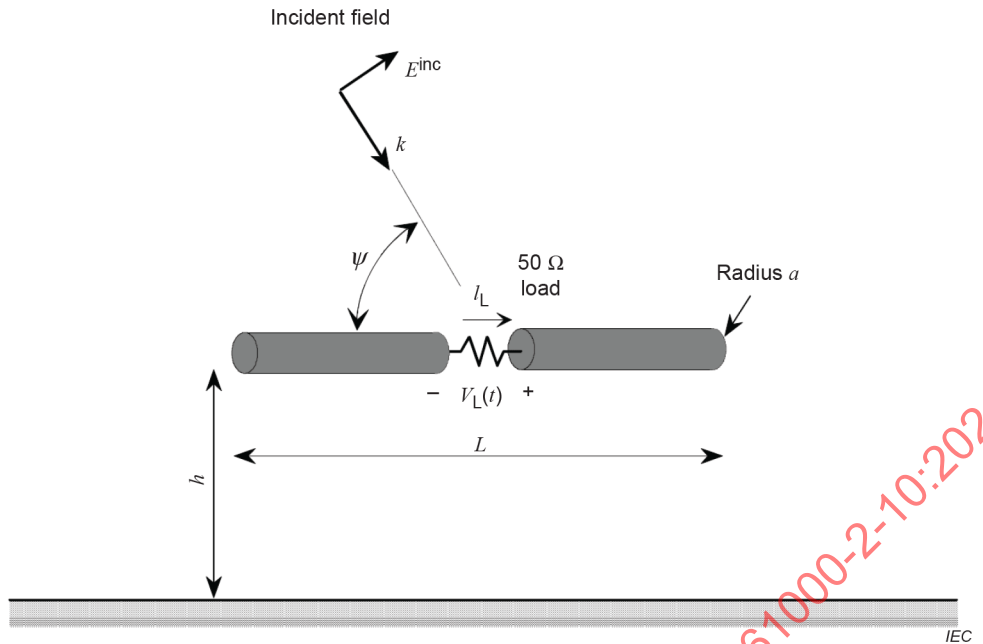


Figure C.4 – Geometry of the dipole antenna

The presence of the ground plane has caused another parameter to be needed in describing the geometry – namely the height of the antenna over the ground, h . As noted in Formula (C.6), the excitation of the antenna arises from the incident field plus a ground-reflected contribution. Typically, the ground-reflected excitation tends to induce an antenna response that cancels the response induced by the incident field. However, this cancelling excitation contribution usually arrives at the antenna after the first peak in the response has occurred. Thus, the earth-reflected field often has no impact on the peak values of the response for antennas that are higher than $L/2$ over the ground. Therefore, a good estimate of the worst case response of the antenna is provided by neglecting the ground reflection completely, and treating the antenna as if it were in free-space. This is certainly reasonable, as these types of antennas are usually located far from the earth in order to optimize their in-band operational characteristics.

Calculations for the CPDs of the dipole antenna responses are carried out in the same way as for the monopole antenna, except that the variations of the angle ϕ shall also be taken into account. This is done by assuming that for a fixed antenna direction (along the x -axis), the angle ϕ can take any value between 0° and 360° with equal probability. For these calculations, a total of 3 000 antenna locations within the illuminated region were used, with a total of 500 values of ϕ being used for each antenna location. This required a total of 1,5 million coupling cases to be considered to generate the probability curves.

C.4 Calculated results

Using the previously discussed analysis procedure and numerical models, the CPDs for the four antenna responses to the IEC early-time HEMP environment have been calculated for both antenna types. For this study, four different values of length L have been used: $L = 1$ m, 3 m, 10 m and 100 m for both the monopole and the dipole antennas. These results are presented in Clause C.4.

The computed CPDs for the vertical monopole antenna load currents and voltages are presented in Figure C.5, Figure C.6, Figure C.7, and Figure C.8, for the four different monopole lengths.

Similarly, the CPDs for the horizontal dipole antenna load currents and voltages are presented in Figure C.9, Figure C.10, Figure C.11, and Figure C.12, for the four different dipole lengths.

C.5 Summary of results

The probability curves of Figure C.5 through Figure C.12 provide significant detail as to the possible antenna behaviour subject to HEMP excitation. Frequently, however, only the responses for the 50 %, 10 % and 1 % cumulative probability levels are desired. These are referred to in this document as the 50 %, 90 % and 99 % "severity levels", respectively, which indicate the percentage of antenna cases having a response less than the indicated response level. These values can be found in Table 3 to Table 9.

All of these results have been calculated for an antenna parameter $\Omega_0 = 8$, which corresponds to an L/a ratio of 27,3 for the monopole and an L/a ratio of 54,6 for the dipole. If a different aspect ratio for the antenna is desired, the antenna responses would change. Figure C.13 presents multiplicative correction factors, normalized to unity for $\Omega_0 = 8$, which can be applied to the data of Annex C, and Table 4 to Table 9, to yield data for different antennas.

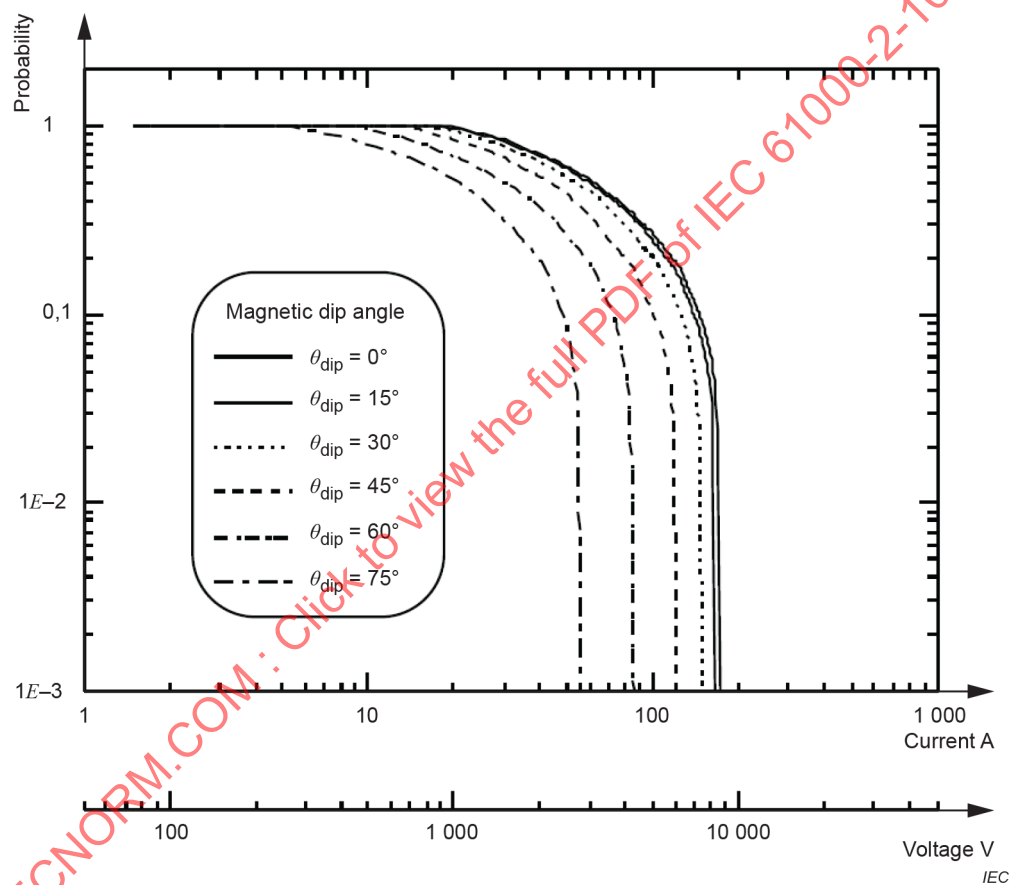


Figure C.5 – Cumulative probability distributions for the peak responses for the 1 m vertical monopole antenna load currents and voltages

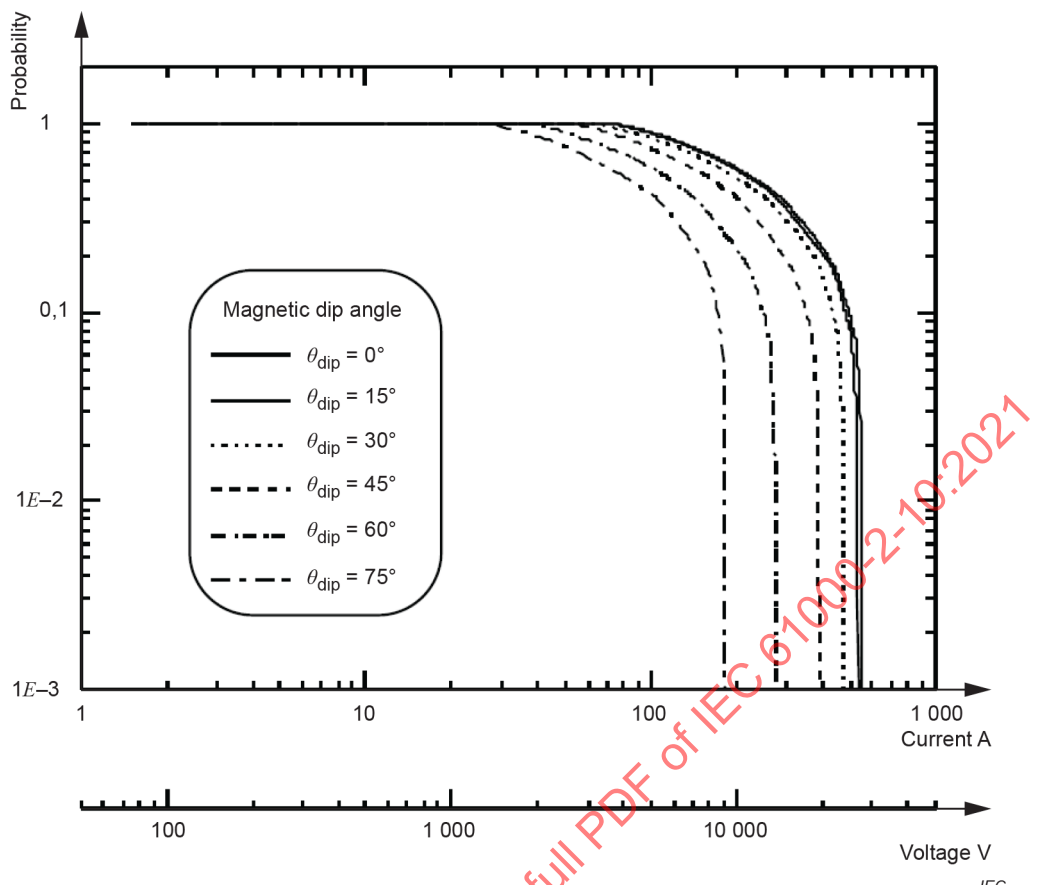


Figure C.6 – Cumulative probability distributions for the peak responses for the 3 m vertical monopole antenna load currents and voltages

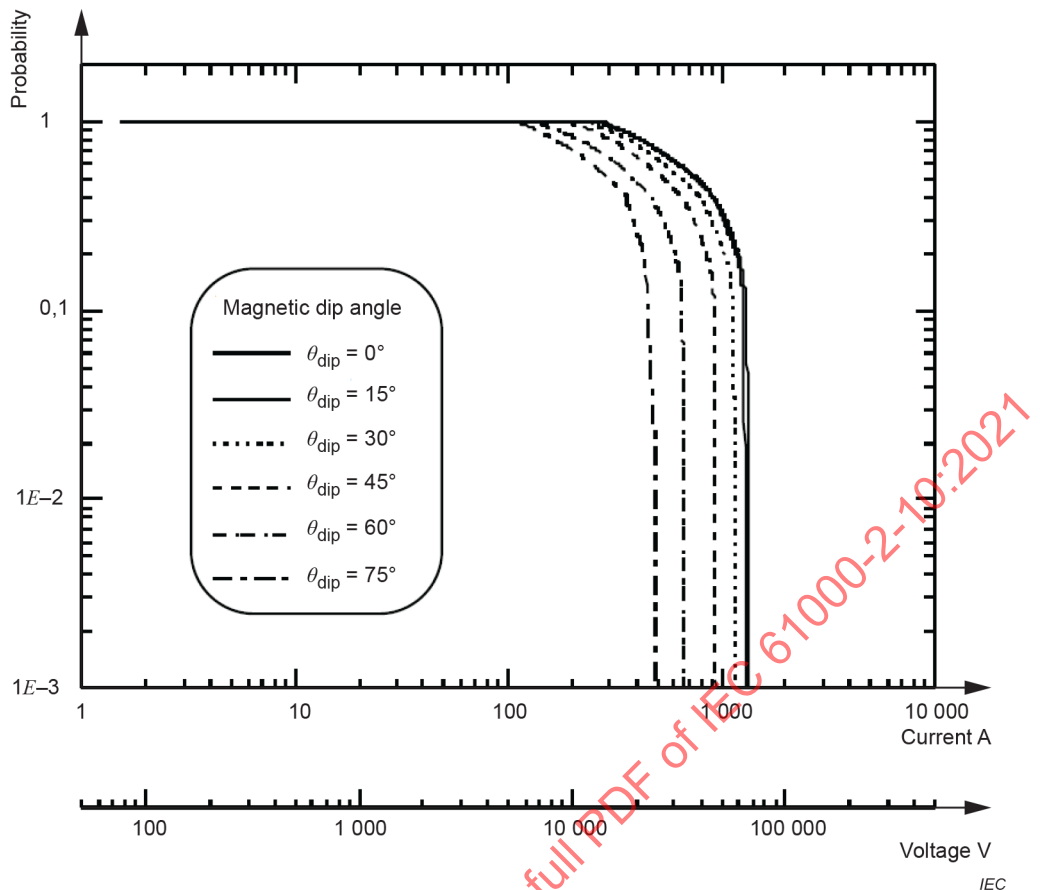


Figure C.7 – Cumulative probability distributions for the peak responses for the 10 m vertical monopole antenna load currents and voltages

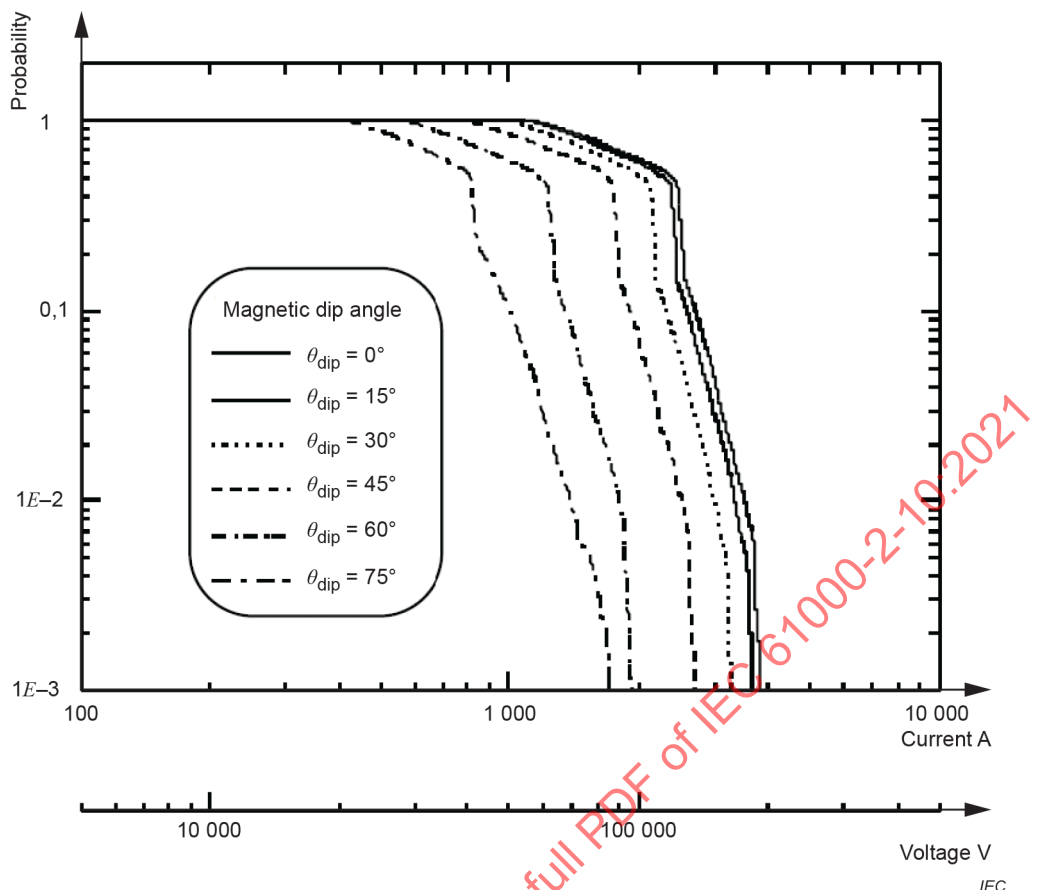


Figure C.8 – Cumulative probability distributions for the peak responses for the 100 m vertical monopole antenna load currents and voltages

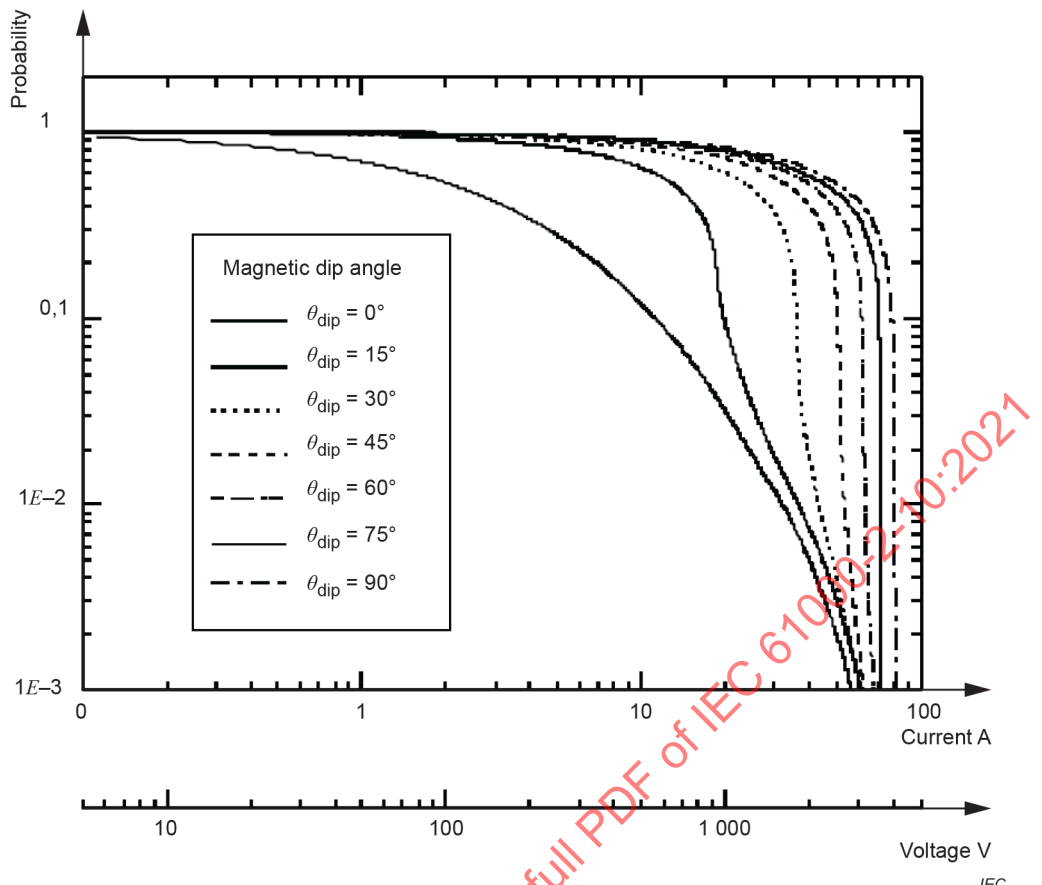


Figure C.9 – Cumulative probability distributions for the peak responses for the 1 m horizontal dipole antenna load currents and voltages

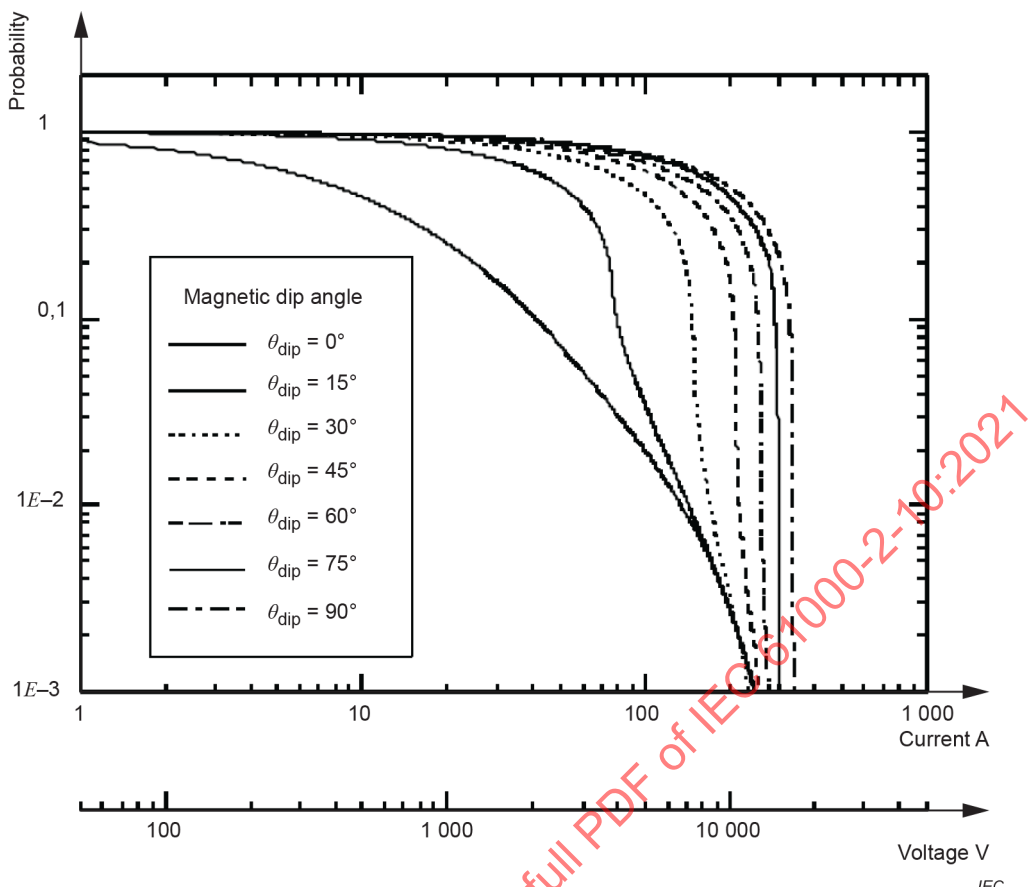


Figure C.10 – Cumulative probability distributions for the peak responses for the 3 m horizontal dipole antenna load currents and voltages